On the geometry of demixing: A study of lipid phase separation on curved surfaces

Rinaldin, M.

CHAPTER 5

LIPID DEMIXING ON SUBSTRATES TOPOGRAPHICALLY PATTERNED WITH COLLOIDS

Here, we fabricate supported lipid bilayer (SLBs) of varying lipid composition and curvature by using substrates which are topographically patterned with colloidal particles as a scaffold. We observe that both the curvature and lipid composition determine whether the system is phase-separated, where the lipid domains are localised, and that these features are strikingly different from the case in which the membrane is supported only by colloidal particles in solution. Our results provide a reference for a quantitative interpretation of previous experiments on curved SLBs on topographically patterned substrates and shed new light on the effect of lipid exchange in phase-separated lipid membranes and two-dimensional systems in general.

This chapter is based on:

M. Rinaldin, P. Fonda, L. Giomi, and D. J. Kraft, Geometric pinning in curved scaffolds connected to a reservoir, *in preparation*.

5.1 Introduction

In Chapter 3, we investigated the role of curvature on liquid-liquid phase separation (LLPS) of lipid membranes. To do this, we fabricated lipid membranes on colloidal particles, so-called colloid supported lipid bilayers (CSLBs). In these systems, the lipid composition of the membrane was conserved, or in other words, there was no exchange of lipids with the surrounding. This is ascribed to the fact that colloidal particles possess a closed surface, *i.e.* a surface that is compact and does not have boundaries. We argued that the surface closeness has significant consequences on the partitioning of the lipids in domains and their assembly into microscopic patterns, including geometric pinning for small concentration of unsaturated lipids and the presence of curvature-induced lipid sorting. Do these phenomena persist if the membrane is open?

To answer this question, we present here a model system *in vitro* in which we open the membrane on the colloids by connecting it to a reservoir of lipids. To do this, we fabricate supported lipid bilayers on substrates topographically patterned with colloidal particles, *i.e.* surfaces onto which we attach colloids. In this way, the lipid membrane on the flat substrate acts as a reservoir of lipids for the lipid membrane on the colloids and we can test the effect of local lipid exchange experimentally.

The chapter is organised as follow. First, we describe the experimental set-up, then we study the phase separation patterns as a function of lipid composition on topographically patterned substrates with spherical and dumbbell-shaped particles. Finally, we complete the comparison of the open system introduced here with the CSLBs in Chapter 3.

5.2 Methods

5.2.1 Reagents. The lipids 1-palmitoyl-2-oleoyl-*sn*-glycero-3-phosphocholine (POPC), porcine brain sphingomyelin (BSM), ovine wool cholesterol (chol), 1,2-dioleoyl-*sn*-glycero-3-phosphoethanolamine-N-lissamine rhodamine B sulfonyl 18:1 (Liss Rhod PE), N-[11-(dipyrromethene boron difluoride)undecanoyl]- Derythro- sphingosylphosphorylcholine (C11 TopFluor SM), and 1,2-dioleoyl-sn-glycero-3-phosphoethanolamine-N--[methoxy(polyethylene glycol)-2000] (DOPE-PEG(2000)) were purchased from Avanti Polar Lipids and stored at $-20\,^{\circ}\mathrm{C}$. HEPES buffer was made with 115 mM NaCl, 1.2 mM $CaCl_2$, 1.2 mM $MgCl_2$, 2.4 mM K_2HPO_4, and 20 mM HEPES, all purchased from Sigma Aldrich. All chemicals were used as delivered.

5.2.2 Substrates and colloids. Borosilicate glass coverslips, 1 mm thick, were purchased from VWR international. MICA substrates were purchased from Agar Scientific. Silica spheres were purchased from Microparticles GmbH, $(2.06 \pm 0.05)\,\mu\mathrm{m}$ and $(7.0 \pm 0.3)\,\mu\mathrm{m}$ in diameter, and Fluka $(3.0 \pm 0.3)\,\mu\mathrm{m}$ in diameter. Polystyrene-3-(Trimethoxysilyl) propyl methacrylate (PS-TPM) symmetric dumbbell and asymmetric dumbbell-shaped particles were synthesised by making a protrusion on swollen PS-TPM particles[133]. The symmetric dumbbell-shaped particles have a total length of $(5.23 \pm 0.05)\,\mu\mathrm{m}$, the ratio between the diameters of the two lobes equals 0.98 ± 0.04, and the smaller lobe diameter equals $(2.68 \pm 0.04)\,\mu\mathrm{m}$ (Figure 3.1d). The asymmetric dumbbell-shaped particles have a total length of $(4.01 \pm 0.04)\,\mu\mathrm{m}$, the ratio between the

diameters of the two lobes equals 0.57 ± 0.02, and the smaller lobe diameter equals (1.45 ± 0.03) μm. Hematite cubic particles were made following Sugimoto *et al.*[194], coated with silica[37] and treated by HCl to remove the hematite core to obtain cubic shells with a resulting corner-to-corner distance of (1.76 ± 0.08) μm, and an m-value of 3.3 ± 0.6. For more details about the synthesis of the particles, see Section 3.2.2, in Chapter 3.

5.2.3 Sample preparation.

Substrates

Particular attention was given to the cleaning of the substrates since it strongly influences the formation of the bilayer. Glass coverslips were cleaned by sequential sonication in 2 % w/w Hellmanex solution in MilliQ water, ethanol, and MilliQ water. The coverslips were kept in MilliQ water for a maximum of three days to keep them hydrophilic. MICA substrates were cleaned by sequential sonication in acetone, ethanol, and MilliQ water.
All particles were washed three times in MilliQ water before being used in the lipid coating experiments. To attach the colloids to a substrate, a solution of particles was dried on the glass coverslip. Since the particles experience strong capillary forces during the drying process, they often form clusters. To suppress aggregation, we use diluted dispersions of particles, namely ≈ 50 μL of 5 gL^{-1} colloid solution for each coverslip. In the experiments with cubic particles, we heated the sample to 500°C to burn the polymers used for stabilisation of the cubic colloids, as shown in Chapter 2. In some experiments with symmetric and asymmetric dumbbells and spheres, we also calcinated the particles at 500 °C to remove the inner polymer network of polystyrene and TPM. We did not see a difference in results between dumbbells that underwent temperature treatment and dumbbells that did not, except that the silica shell was sometimes broken after calcination.

Supported lipid bilayers

A mixture of 500 μg of POPC, BSM, and chol in different mole ratios with 0.2% DOPE-Rhodamine, 0.2% C11 TopFluor SM, and 5% DOPE-PEG(2000) in chloroform was prepared and the chloroform was evaporated in a vacuum chamber for 2 hours. The lipids were dispersed in HEPES buffer to 2 gL^{-1} concentration, and left self-assembling into multi-lamellar vesicles during 30 minutes of vortexing. The solution was heated in an oven to 70 °C, and then extruded 21 times with a mini-extruder (Avanti Polar Lipids) placed on a heating plate set at 70°C equipped with two 250 μL gas-tight syringes (Hamilton), four drain discs, and one nucleopore track-etch membrane with 0.03 μm pores diameter (Whatman). Then, 50 μL of the resulting small unilamellar vesicles (SUVs) solution together with 1 mL of HEPES buffer was added to a holder with the topographically patterned substrate and put in the oven at 70°C for one hour. After that, the sample was rinsed three times with HEPES buffer, to remove excess SUVs in solution. During each step described above, samples were covered by aluminium foil to prevent bleaching of the dye and oxidation of unsaturated lipids.

5.2.4 Sample characterisation. The samples were imaged at room temperature with an inverted confocal microscope (Nikon Eclipse Ti-E) equipped with a Nikon A1R confocal

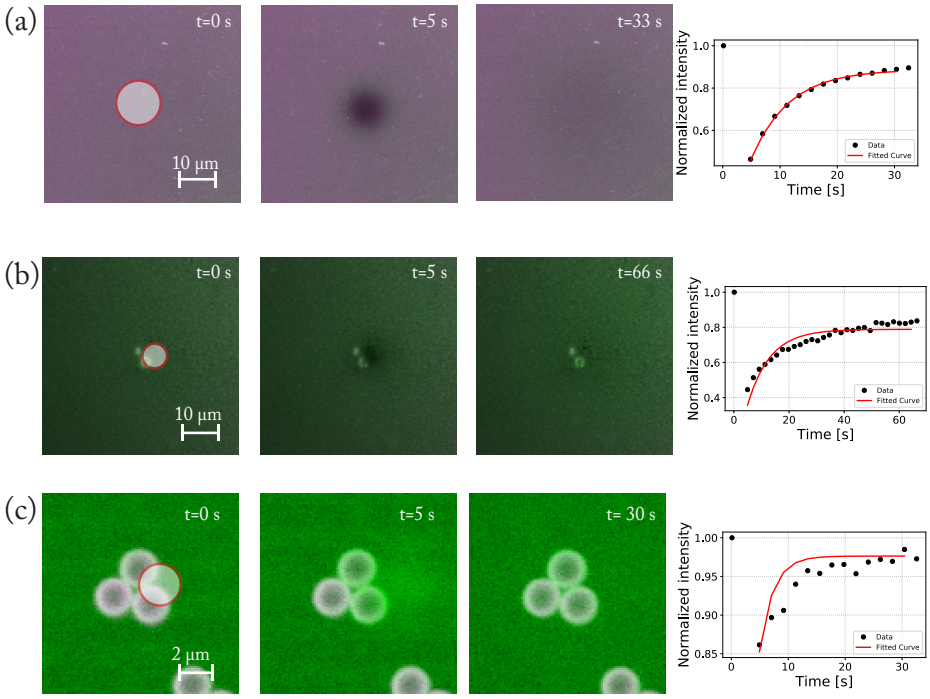

Figure 5.1: Fluorescence recovery after photo-bleaching (FRAP) experiment on a bilayer (a) on a flat glass substrate, **(b)** in the contact area between substrate and colloid, and **(c)** on a colloid. From left to right: image sequences before bleaching, after bleaching, and at the end of the experiment when the signal was recovered, are reported. The bleaching areas are indicated in red. On the right, the data and the recovery curves of DOPE-Rhodamine are shown.

scan head with Galvano and resonant scanning mirrors. A 100x oil immersion objective (NA=1.4) was used. 488 and 561 nm lasers were used to excite C11 TopFluor and Lissamine Rhodamine dyes, respectively. The laser beams were passed through a quarter-wave plate to avoid polarisation of the dyes, and the emitted light was separated using 500-550 nm and 565-625 nm filters, respectively. The mobility of the bilayer on the colloids, on the substrates and in the contact area between the substrate and the colloid was tested by fluorescence recovery after photobleaching (FRAP) experiments which are reported in Figure 5.1. Three-dimensional image stacks were acquired by scanning the sample in the z-direction with an MCL Nano-drive stage and reconstructed with Nikon AR software.

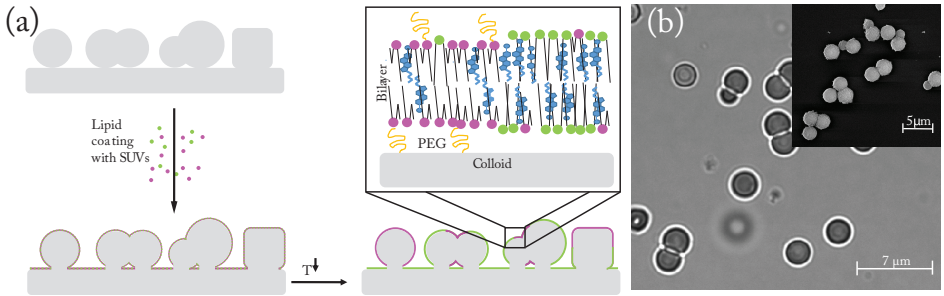

Figure 5.2: SLB on substrates topographically patterned with colloidal particles. (a) Overview of the experimental set-up. Colloids with a silica surface and different shapes are deposited onto a glass coverslip. At 70 °C the colloids and the substrate are coated with a lipid bilayer by deposition of small unilamellar vesicles (SUVs). Upon lowering the temperature, the lipid bilayer undergoes phase separation. The lipids in blue, green and magenta are cholesterol, SM, and POPC, respectively. Polyethylene glycol molecules (PEG) are shown in orange. The LO and LD phases are represented in green and magenta, respectively. **(b)** Light microscopy image of a topographically patterned substrate with symmetric and asymmetric dumbbell-shaped colloids. In the inset, scanning electron microscopy image (SEM) of the same substrate.

5.3 Results and discussion

In CSLBs, lipid domains arrange in equilibrium configurations which are determined by the interplay between the total lipid composition of the membrane and the shape of the colloid, as seen in Chapter 3. To study how these equilibrium configurations are affected by lipid exchange, we present here an experimental set-up in which the lipid composition is not conserved in the neighbourhood of the colloid. To do so, we fabricate substrates topographically patterned with colloidal particles and then coat them with a multicomponent lipid bilayer. In this way, lipids can exchange between colloids and the flat substrate. Thus, the membrane on the substrate can be interpreted as a reservoir of lipids for the membrane on the colloids. We want to stress that while there is lipid exchange between the membrane on the colloid and the substrate, the total lipid composition of the whole SLB is conserved. Moreover, we will show in the following section how the total lipid composition affects phase separation and in particular geometric pinning.

5.3.1 The experimental system. Substrates topographically patterned with colloids of spherical, cubic, symmetric and asymmetric dumbbell shape were lipid-coated by deposition of small unilamellar vesicles (SUVs)[29] made from a ternary mixture of the lipids POPC, BSM, and cholesterol in different mole ratios. To increase the thickness of the water layer between the surface of the particle and the bilayer, 5% mole ratio of PEGylated lipids DOPE-PEG(2000) was included. In this way, we could improve the mobility of the bilayer on rough silica surfaces. To image the liquid-disordered (LD) and the liquid-ordered (LO) phases 0.2 % of fluorescent lipids DOPE-Rhodamine and C11 TopFluor SM were used. In the following images, these phases are shown in magenta and green,

respectively. The lipid coating was performed above the critical transition temperature to keep both lipid bilayer and SUVs in the mixed state. Phase separation was then induced upon cooling. An overview of the experimental set-up is shown in Figure 5.2a. The lipid mobility on the colloids, on the substrate, and at the edge between the colloids and the substrate was tested by FRAP experiments, of which some examples are reported in Figure 5.1. From these measurements, we conclude that the lipid bilayer is fluid everywhere on the surface.

5.3.2 The ternary phase diagram of a SLB on a substrate with spherical colloids. It is known from experiments with giant unilamellar vesicles (GUVs) that the lipid composition affects the phase diagram of multicomponent lipid membranes[11]. However, no similar investigation has been done on SLBs. Here, we study the phase behaviour dependency on the total lipid composition of the SLB by varying the mole ratio between POPC, BSM, and cholesterol. To visualise this, we used a ternary phase diagram.

In Figure 5.3a the phase diagram of a SLB on a substrate topographically patterned with spherical colloids is shown together with the three-dimensional reconstructions of sections of bilayers representative of the samples. Figure 5.3a shows that, depending on the total lipid composition, the SLB can be mixed or phase-separated. We note that we did not study lipid mixtures with more than 50% of cholesterol because such high concentrations of cholesterol form a crystal phase. The formation of crystals in samples with high concentration of cholesterol was visible already during the dispersion of the lipids in HEPES in the form of macroscopic clusters.

The phase separation region occupies the central part of the ternary diagram, as observed in experiments with GUVs with the same[135] or similar[11] lipid composition. In confocal microscopy images, the mixed state appears white, because the signal from the magenta and the green channel completely overlap due to co-localisation of the dyes (left inset of Figure 5.3a). In the phase-separated state, the LD phase preferentially covers the whole colloid and the LO phase is preferentially localised on the flat substrate (right inset of Figure 5.3a). This is due to geometric pinning: the softer LD phase is pinned to regions where the curvature is different from zero, that is where the colloids are. The more rigid phase, on the other hand, is localised where the curvature is equal to zero.

Subramaniam *et al.*[5] reported a comparable result in experiments with SLB on patterned PDMS substrates of half-spheres. They showed that the softer LD phase was pinned on the half-spheres for a single lipid composition. While our results agree with this earlier work, they are also surprising. Since on a flat surface phase separation inevitably implies the formation of circular domains for liquid-liquid phase separation and ramified domains for solid-liquid phase separation, we expected to observe microscopic domains also in the bilayer on the glass, but this did not happen. Instead, we observed the geometrically pinned configurations shown in the insets in Figure 5.3 for different lipid compositions. This implies that the relative ratio of lipids going into one phase between the membrane on the colloid and the membrane on the flat substrate must change depending on the total lipid composition of the SLB.

Only after five days, we observed a few microscopic circular domains (Figure A.3d, in the Appendix). The absence of microscopic circular liquid domains on glass was recently

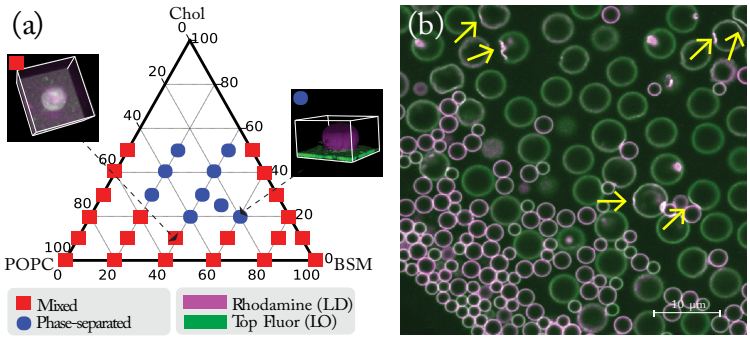

Figure 5.3: Demixing on a substrate topographically patterned with colloidal spheres. (a) Ternary phase diagram of a lipid bilayer on a substrate topographically patterned with colloidal spheres. Depending on the overall composition, the membrane can be in the mixed state (red squares) or in the phase-separated state (blue circles). In the insets, three-dimensional reconstructions of the bilayer in the mixed (left) and in the phase-separated (right) state are shown. The LD and the LO phase are represented in magenta and green respectively. **(b)** View of the equatorial plane of a lipid bilayer supported on a plane with spherical colloidal particles of three different sizes. The LD phase is preferentially localised on spheres with higher curvature, *i.e.* smaller radii, and on the dimples highlighted with yellow arrows.

explained by Goodchild *et al.*[195]. They found that microscopic solid and liquid domains cannot be formed in SLBs on glass, because the nanoscopic roughness of fused glass hinders coalescence of sub-micron sized domains.

However, interestingly, in our experiments, we do observe microscopic domains on the colloids. We believe that this is due to two effects. First, in Chapter 3, we showed that microscopic phase separation occurs on colloids with a silica surface, implying that the surface of the colloids allows for the fusion of nanoscopic domains. Second, curvature can induce phase separation. In previous experiments with manipulated vesicles[7] and CSLBs (Chapter 3), it was observed that curvature can promote phase separation. Specifically, Sorre *et al.*[7] showed that in tubes pulled from GUVs unsaturated lipids partition in higher ratios into the more curved tubes. Similarly, we showed in Chapter 3 that phase separation likelihood increases with curvature. We note that we observed micrometre-sized circular liquid domains in SLBs supported by MICA, as suggested by Goodchild *et al.*[195]. We report the results in the Appendix, Figure A.3e-f.

To test if the curvature modulus affects phase separation in the system, a topographically patterned substrate with spheres of different diameters, namely (2.06 ± 0.05) µm, (3.0 ± 0.3) µm and (7.0 ± 0.3) µm, was used. Interestingly, the curvature of the spheres strongly influences the preferential partitioning of the lipids. Figure 5.3b shows that the smaller spheres are covered by more LD phase than the larger spheres to the extent that on the largest spheres, the geometric pinning effect disappears. In the same figure, some of the 7 µm spheres present dimples on the surface, probably due to synthesis or degradation. Strikingly, on the dimples, the membrane is in the LD state. This indicates that negative

curvature pins the softer LD phase.

We note that geometric pinning of the LD phase in the contact area between the colloid and the flat glass was expected because this region has high curvature. However, we rarely observed pinning at the edge between the substrate and the particle (Appendix, Figure A.3a-c). Therefore, we hypothesise that at the edge, the SLB might be pulled from the substrate, decreasing the local membrane curvature.

While examining the lipid-coated substrate with spherical colloids, some dumbbell-shaped particles (Figure 5.4a) were also found. These particles are the result of silica spheres aggregating during the synthesis process. Interestingly, strong geometric pinning occurs on their waist. The three-dimensional reconstruction of the membrane in Figure 5.4b shows that the LD phase is localised on the neck of the dumbbell, where the curvature of the membrane is the highest, while the rest of dumbbell and substrate are covered by the LO phase. This configuration, when compared with the one of the spheres and previous experiments[5], hints at strong geometric pinning by high curvature regions.

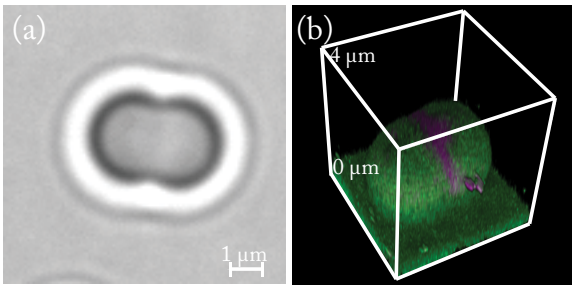

Figure 5.4: The liquid-disordered phase pinned at the neck. (a) Light microscopy image of a dumbbell-shaped colloid resulting from the silica sphere synthesis. **(b)** Three-dimensional fluorescence reconstruction of the bilayer on such a dumbbell.

The SLB in Figure 5.4b was made with a specific lipid composition, namely a mixture of 50% BSM, 25% POPC, and 25% cholesterol. Since we found that the lipid composition influences phase separation in SLBs on substrates topographically patterned with spheres, we will now study how anisotropic colloids affect the phase separation landscape.

5.3.3 The ternary phase diagram of a SLB on a substrate with dumbbell-shaped colloids. To quantitatively study how lipid composition affects phase separation on anisotropic surfaces, we used substrates topographically patterned with dumbbell-shaped particles.

For this experiment a high yield of dumbbells of controlled geometry was necessary, therefore we synthesised dumbbell-shaped colloids and used them to pattern the substrate. See Figure 5.2b for an image of the colloids on the substrate. The dumbbells were obtained by creating a protrusion on PS-TPM spheres, coating them with silica, and calcinating them for SLB formation. Both symmetric and asymmetric dumbbell-shaped particles were used to study the effect of asymmetry of the topographical features on phase separation. This allows us to compare the results directly with the results obtained on CSLBs. As we did previously for substrates made with spherical colloids, we also investigated the effect of lipid composition on phase separation by using a ternary phase

diagram.

Figure 5.5a can be directly compared with the ternary phase diagram of the SLB on the substrate patterned with spheres in Figure 5.3a. In both diagrams, the mixed phase occupies the lower part and the borders of the phase diagram. However, the inhomogeneous curvature of the dumbbells *versus* the homogeneous curvature of the spheres leads to a more complex phase diagram for the SLB on the substrate topographically patterned with dumbbells, namely two types of equilibrium states instead of one. The cholesterol concentration appears to be the critical parameter regulating the switching between the two states. This is not unexpected as cholesterol has been previously found to influence domain size[196].

As can be seen from three-dimensional reconstructions of the bilayer on asymmetric dumbbells, the additional asymmetry between the two types of employed dumbbells does not influence the ternary phase diagram. Therefore it can be concluded that the difference in the curvature of the two lobes in the asymmetric dumbbell is not sufficiently high to induce further curvature effects in the ternary phase diagram. Nevertheless, we will report in the next section how this curvature difference additionally affects the system.

To conclude this part, we want to stress that both types of phase-separated states show regular and systematic geometric pinning. In particular, Figure 5.5b shows that the (contour) fraction occupied by the LD phase on both the symmetric and asymmetric dumbbells seems to be constant. In the next section, we will measure this quantity and compare it for symmetric and asymmetric dumbbells. Even more surprising, the size of the region occupied by the LD phase on the neck of the dumbbells does not change with the lipid composition. We will also quantify this phenomenon in the next section.

Note that some shells were broken, during calcination (yellow arrows in Figure 5.5b). When the colloids are broken, the LD phase is localised at the highly curved edges.

5.3.4 Quantification of geometric pinning in symmetric and asymmetric dumbbells. Figure 5.5b suggests that the localisation of the LD phase on the neck of the symmetric and asymmetric dumbbells occurs in a regular way, or, in other words, the area fraction occupied by the LD phase appears to be constant. To investigate this, the area fraction occupied by the LD phase on 200 colloidal particles of symmetric and asymmetric dumbbell shape made with a fixed lipid composition, namely 50% BSM, 25% POPC, and 25% cholesterol was measured. For each dumbbell, the fraction of the contour occupied by the soft phase was found by analysing the normalised fluorescence intensity profile of the equatorial plane of the colloids. In Figure 5.6a and d, fluorescence images of the equatorial plane of symmetric and asymmetric dumbbell-shaped particles are shown. In Figure 5.6b and e, the normalised intensity profile of the Rhodamine dye labelling the LD phase is plotted with the mean curvature. From the figures, we can observe that at the neck, where the mean curvature is high, the intensity of the dye labelling the LD phase shows a peak. Assuming that the LD domain is axisymmetric, the contour fraction can be converted into a surface fraction. Figure 5.6c and f show the probability density function (PDF) of the surface fraction occupied by the LD phase for the symmetric and asymmetric dumbbell, respectively. In both cases, the PDF follows a Gaussian distribution indicating that geometric pinning is regular. By fitting the data with a Gaussian function,

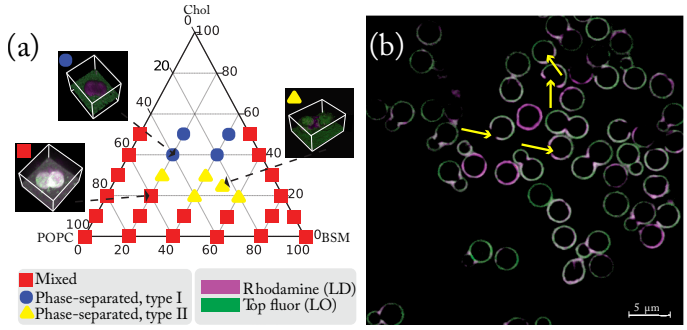

Figure 5.5: Demixing on a substrate topographically patterned with colloidal dumbbells. (a) Ternary phase diagram of a lipid bilayer on a substrate topographically patterned with dumbbell-shaped particles. In the insets, three-dimensional reconstructions of the bilayer in the mixed and in the phase-separated (geometrically pinned) states are shown. **(b)** View of the equatorial plane of a lipid bilayer supported on a plane with symmetric and asymmetric dumbbell-shaped colloids. The LD phase is preferentially localised on the neck of the dumbbells. In this image the scaffold was calcinated at 450 °C and in some cases the silica shell is broken (yellow arrows).

we found that the fraction of the surface of the particles occupied by the LD phase is $31 \pm 9\%$ for symmetric dumbbells and $27 \pm 10\%$ for asymmetric dumbbells. Since these measurements agree within error, we do not observe any effect of the lobe's curvatures. However, for asymmetric dumbbells, we measured the area fraction occupied by the LD phase (A_{LD}) on the smaller and the larger lobe with respect to the whole colloid (Figure 5.6g), or with respect to the individual lobes (Figure 5.6h). With respect to the whole colloid, A_{LD} is smaller for the smaller lobe than for the larger lobe, as expected by size arguments. However, with respect to the respective lobes, A_{LD} is higher on the smaller lobe than on the larger lobe. This can be understood by considering that the smaller lobe has higher curvature, and therefore it pins relatively more LD phase than the larger lobe. This effect is induced only by the difference in curvature between the two lobes in the asymmetric dumbbells and disappears for symmetric dumbbells where the LD phase is equally distributed between the two lobes.

To test if the total lipid composition affects the value of A_{LD}, A_{LD} was measured for 50 symmetric dumbbells made of two different SLB lipid compositions, namely BSM:POPC:Chol=40:20:40 and 20:50:30. The resulting values of preferred area fraction from the Gaussian fit are $26 \pm 6\%$ and $26 \pm 4\%$, respectively. We plot the probability density functions of these area fractions with the one calculated before for the lipid mixture BSM:POPC:Chol=50:25:45 in Figure 5.7. Since the measurements agree within the error, we conclude that the size of the LD domain on the neck of the dumbbell is not affected by the tested SLB composition.

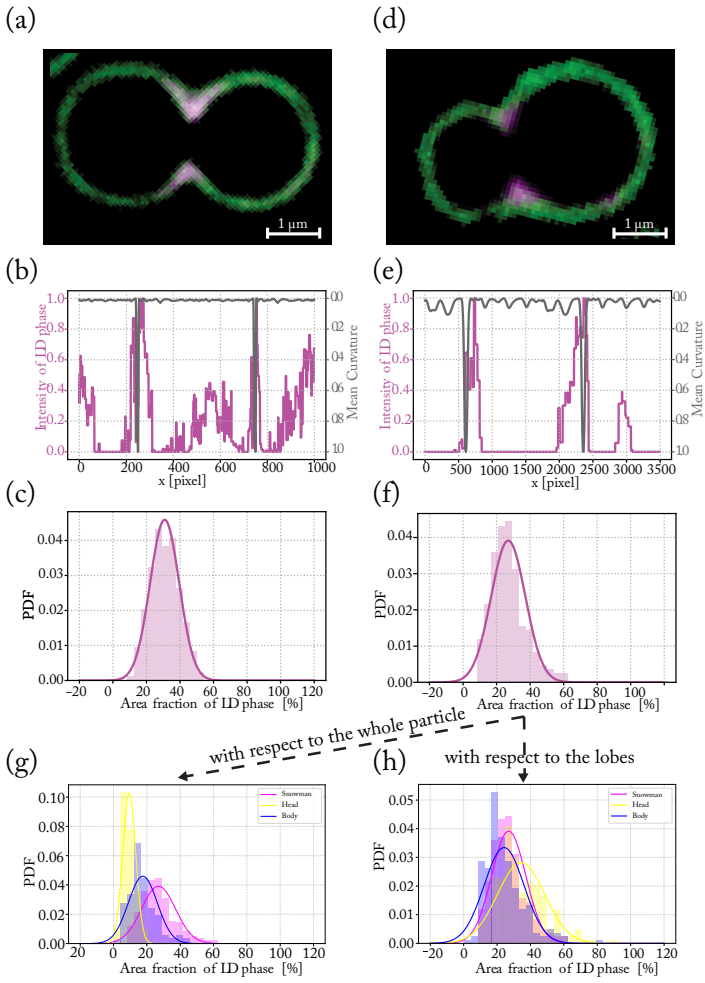

Figure 5.6: Quantification of area fraction occupied by LD phase in symmetric and asymmetric dumbbells. Fluorescence microscopy image of the equatorial profile of a membrane on an symmetric **(a)** and asymmetric **(d)** dumbbell-shaped colloid. Plot of the normalised fluorescence intensity of the Rhodamine dye that labels the LD phase (magenta curve) and of the normalised mean curvature (gray curve) measured along the profile for symmetric **(b)** and asymmetric **(e)** dumbbells. Probability density function (PDF) of area fraction occupied by LD phase for the symmetric **(c)** and asymmetric **(f)** case fitted with Gaussian curves. PDF of area fraction occupied by LD phase in asymmetric dumbbells calculated with respect to the whole colloid **(g)**, and to the individual lobes **(h)**.

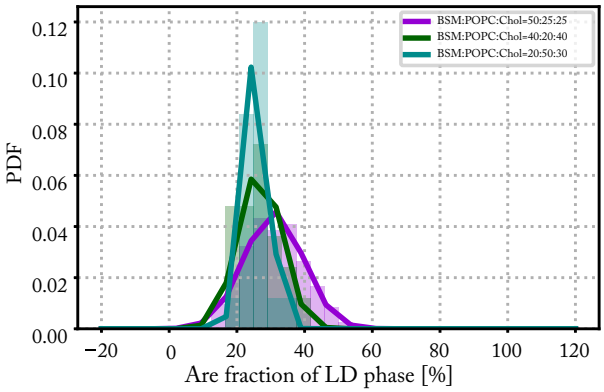

Figure 5.7: PDFs of area fraction covered by the LD phase on symmetric dumbbells on SLBs made from three different compositions. The three PDFs show that the average values of percentage of area fraction occupied by the LD phase are 31 ± 9%, 26 ± 6%, and 26 ± 4% for lipid mixtures made of BSM:POPC:Chol= 50:25:25 (on 200 particles), 40:20:40 (on 50 particles), and 20:50:30 (on 50 particles), respectively.

5.3.5 The effect of local lipid exchange. By comparing these results with the work on CSLBs (Chapter 3), we conclude that allowing lipid exchange between the bilayer on the colloids and the reservoir (flat SLB) strongly affects the phase separation configurations. To demonstrate this, we report in Figure 5.8 a sample in which the same particles are in one part CSLBs (region "a") and in another topographical features of a SLB (region "b"). The bilayer in region "a" is in the mixed state, while the bilayer in region "b" is phase-separated with the LD phase localised on the colloid and the LO phase localised on the flat substrate.

To complete the comparison with the work on CSLBs, a substrate topographically patterned with cubic particles was used. A scanning electron microscopy (SEM) image of the particles and fluorescence images of the SLB are reported in Figure 5.9. Similarly to what has been observed in experiments with CSLBs, Figure 5.9 shows that the inhomogeneous curvature of the cubes, attributable to the presence of edges and corners, competes with the minimisation of the interface. However, the curvature is not strong enough to induce a regular geometric pinning effect such as the one on dumbbell-shaped colloids. As a result, the LD domains randomly localise on the cubes while the flat substrate is preferentially covered by the LO phase.

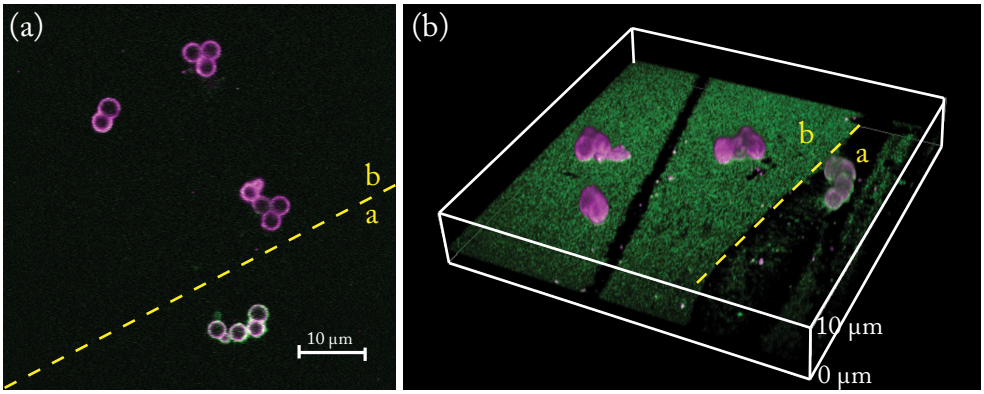

Figure 5.8: The effect of local lipid exchange. (a) Equatorial plane view and **(b)** three-dimensional view of a SLB on a plane topographically patterned with dumbbell-shaped particles. The bilayer on the colloid is in the mixed state (region "a"), while the bilayer on the substrate with colloids connected to the membrane on the substrate (region "b") is in the phase-separated state.

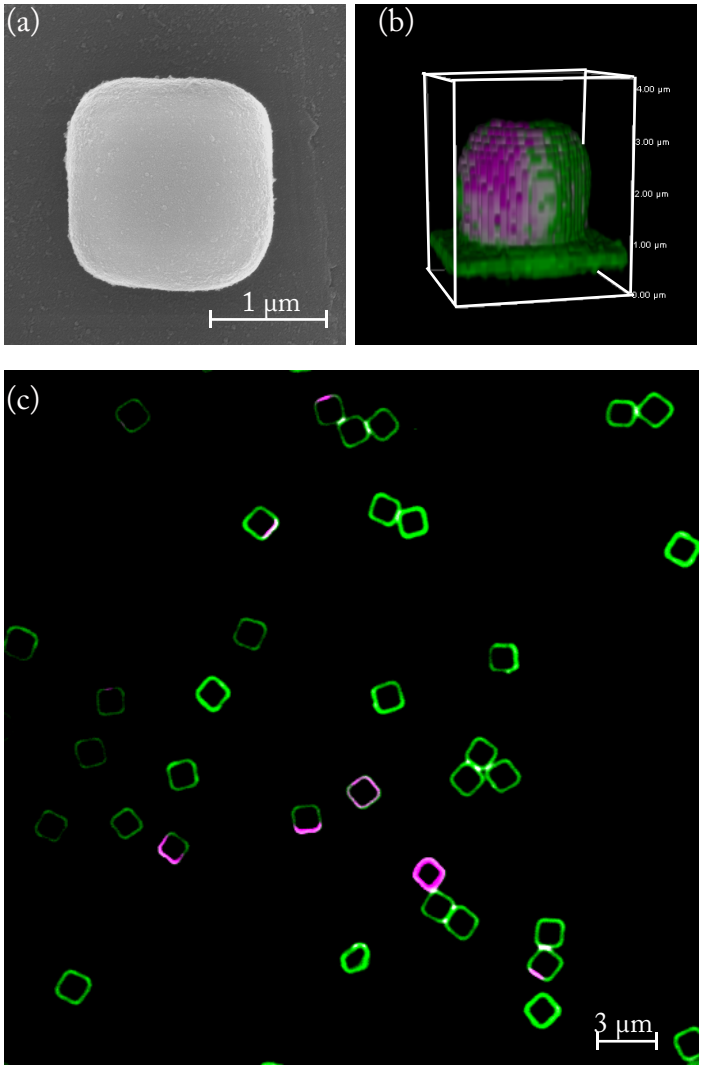

Figure 5.9: Substrate topographically patterned with cubes. (a) SEM image of a colloidal cubic silica shell. **(b)** Three-dimensional reconstruction of fluorescence microscopy image stack of a bilayer supported on a substrate topographically patterned with cubic colloids. The LO phase is preferentially localised on the flat substrate, while, on the colloid, LD lipid domains can be observed. **(c)** Fluorescence microscopy image of the equatorial plane of a lipid bilayer on a substrate topographically patterned with cubic colloids.

5.4 Conclusions

In conclusion, we found that in multicomponent SLBs on topographically patterned substrates with colloidal particles, geometric pinning happens in a regular fashion. Furthermore, its precise manifestation is affected by the total lipid composition of the SLB and the geometry of the patterned substrate.

This result can be directly compared with Chapter 3 to conclude that local lipid exchange induces phase separation and amplifies the geometric pinning effect. This comparison can shed some light on the effect of lipid exchange between highly curved and flat areas in patterned SLBs used in previous experiments[5]. In view of using more complex curved shapes made *via* nanolithography as substrate, it may also help to elucidate the effect of the connection of curved geometries with a flat substrate.

We expect that the accurate determination of the size of the systematically pinned disordered liquid domains can be used in theory and simulations to obtain a measurement of the elastic material properties of the SLB, namely the bending and the Gaussian splay modulus. This can be useful because these quantities are challenging to determine directly *via* experiments with SLBs.

Acknowledgements

I am grateful to Piermarco Fonda for useful discussions. Furthermore, I would like to thank Rachel Doherty and Vera Meester for help with the colloidal syntheses and electron microscopy imaging.